

# Magnetic anisotropy and order parameter in nanostructured CoPt particles

Cite as: Appl. Phys. Lett. **103**, 152404 (2013); <https://doi.org/10.1063/1.4824973>

Submitted: 18 July 2013 . Accepted: 29 September 2013 . Published Online: 11 October 2013

S. V. Komogortsev, R. S. Iskhakov, A. A. Zimin, E. Yu. Filatov, S. V. Korenev, Yu. V. Shubin, N. A. Chizhik, G. Yu. Yurkin, and E. V. Eremin



View Online



Export Citation



CrossMark

## ARTICLES YOU MAY BE INTERESTED IN

[The design and verification of MuMax3](#)

AIP Advances **4**, 107133 (2014); <https://doi.org/10.1063/1.4899186>

[Simple models for dynamic hysteresis loop calculations of magnetic single-domain nanoparticles: Application to magnetic hyperthermia optimization](#)

Journal of Applied Physics **109**, 083921 (2011); <https://doi.org/10.1063/1.3551582>

[Spherical magnetic nanoparticles fabricated by laser target evaporation](#)

AIP Advances **3**, 052135 (2013); <https://doi.org/10.1063/1.4808368>



Learn how to perform the readout of up to 64 qubits in parallel

With the next generation of quantum analyzers on November 17th

Register now



## Magnetic anisotropy and order parameter in nanostructured CoPt particles

S. V. Komogortsev,<sup>1,a)</sup> R. S. Iskhakov,<sup>1</sup> A. A. Zimin,<sup>1</sup> E. Yu. Filatov,<sup>2,3</sup> S. V. Korenev,<sup>2,3</sup>  
 Yu. V. Shubin,<sup>2,3</sup> N. A. Chizhik,<sup>4</sup> G. Yu. Yurkin,<sup>1</sup> and E. V. Eremin<sup>1</sup>

<sup>1</sup>Kirensky Institute of Physics, SB RAS, 660036 Krasnoyarsk, Russia

<sup>2</sup>Nikolaev Institute of Inorganic Chemistry, SB RAS, 630090 Novosibirsk, Russia

<sup>3</sup>Novosibirsk State University, 630090 Novosibirsk, Russia

<sup>4</sup>Siberian Federal University, 660041 Krasnoyarsk, Russia

(Received 18 July 2013; accepted 29 September 2013; published online 11 October 2013)

The correlation of magnetic anisotropy energy with order parameter in the crystallites of CoPt nanostructured particles prepared by thermal decomposition and further annealing has been studied by investigation of the approach magnetization to saturation curves and x-ray powder diffraction pattern profiles. It is shown that magnetic anisotropy energy value in partially ordered CoPt crystallite could be described as an intermediate case between two extremes, corresponding to either single or several c-domains of L1<sub>0</sub> phase in crystallite. © 2013 AIP Publishing LLC. [<http://dx.doi.org/10.1063/1.4824973>]

Huge magnetocrystalline anisotropy in ordered CoPt and FePt alloys makes them good candidates for overcoming the superparamagnetic limit—the main barrier to the progress of magnetic memory development.<sup>1–5</sup> Unfortunately magnetic anisotropy energy (MAE) in CoPt nanoparticles turns out to be much smaller than in the bulk alloys.<sup>6–11</sup> In nanoparticles within the size below 4 nm the MAE reduction is attributed to the thermal instability of ordered L1<sub>0</sub> nanocrystals.<sup>6</sup> In nanoparticles with the size about 10 nm there is no structural and magnetic instabilities, but MAE is still smaller than the bulk value due to the presence of several ordered L1<sub>0</sub> domains inside.<sup>12</sup> Another origin of MAE reduction is the incomplete conversion from A1 to L1<sub>0</sub> structure, i.e., the value of order parameter  $S$  is lesser than 1. The crystal field theory predicts correlation of MAE ( $K$ ) and order parameter as  $K \sim S^2$  for partially ordered homogeneous CoPt alloy.<sup>13–15</sup> The correlation  $K \sim S$  is assumed for the particles with the co-existence of full-ordered L1<sub>0</sub> and disordered A1 regions within one crystalline nanoparticle.<sup>12</sup> The correlation  $K \sim S^2$  has been observed in the bulk crystal in the range of  $S$  from 0.8 to 0.9.<sup>13</sup> However there is still no direct experimental data present on this correlation in CoPt nanoparticles undergoing transformation from A1 to L1<sub>0</sub>. Few reports are available on the dependence of the coercive force in the CoPt and FePt nanoparticles and nanoalloys on the order parameter.<sup>16,17</sup> However, it is hard to use the coercive force value for direct estimation of the magnetic anisotropy energy in nanoparticles because of the interparticle interaction effects. It is appropriate to measure MAE by the methods that are not sensitive to the interparticle interactions, such as the approach magnetization to saturation law in high field regime.<sup>18–22</sup> This paper is devoted to the experimental study of the correlation of magnetocrystalline anisotropy energy and order parameter by means of investigation of the approach magnetization to saturation law in CoPt nanostructured particles.

The samples of equiatomic CoPt nanoparticles were prepared by thermal decomposition of precursor compound

[Pt(NH<sub>3</sub>)<sub>4</sub>][Co(C<sub>2</sub>O<sub>4</sub>)<sub>2</sub>(H<sub>2</sub>O)<sub>2</sub>]·2H<sub>2</sub>O.<sup>23</sup> As-decomposed particles were annealed in helium atmosphere at 400 °C and 500 °C during 2, 4, 8, and 16 h. The CoPt powder was studied over the  $2\theta$  range 5°–120° on a DRON RM4 powder diffractometer equipped with a Cu K $\alpha$  source ( $\lambda = 1.5418 \text{ \AA}$ ) and a graphite monochromator. Silicon powder was used as a line profile standard. Instrumental broadening contribution was modeled using pseudo-Voigt peaks with FWHM's and weight coefficients parameterization according to the Caglioti formula.<sup>24</sup> Indexing of powder diffraction patterns and estimation of unit cell parameters was performed using Fityk<sup>25</sup> software package according to space group constraints. Estimated parameters were then used as initial values for Whole Powder Pattern Modeling (WPPM)<sup>26</sup> procedure using the PM2K package.<sup>27</sup> WPPM is an advanced line profile analysis technique, which allows one to simultaneously take into account various broadening sources. Refinement is performed in terms of real physical parameters—crystalline size distribution, dislocation density, faulting probabilities, etc. Unlike Rietveld method which we have used in the preliminary work,<sup>28</sup> no systematic error arising from choice of arbitrary bell-shaped functions is introduced. To estimate order parameter we use ratio of superlattice ( $h+k+l=2n+1$ ) to fundamental ( $h+k+l=2n$ ) reflection intensities, e.g.,  $I_{(001)}$  to  $I_{(002)}$ . Several pairs of reflections could be used in order to improve accuracy, e.g.,  $I_{(001)}/I_{(002)}$  and  $I_{(003)}/I_{(002)}$ . The order parameter is computed according to the following equation:

$$S = \left( \frac{I_{(001)}}{I_{(002)}} \left( \frac{f_{Co}(s_{002}) + f_{Pt}(s_{002})}{f_{Co}(s_{001}) - f_{Pt}(s_{001})} \right)^2 \right)^{0.5}, \quad (1)$$

where  $s_{hkl} = (\sin \theta_{hkl})/\lambda$ ,  $f(s) = \sum_{i=1}^4 a_i \exp(-b_i s^2) + c$  (atomic scattering factor for the corresponding reflections, which is calculated using interpolation coefficients<sup>22</sup>  $a_i$ ,  $b_i$ , and  $c$ ). Interpolation is valid for Cu K $\alpha$  radiation in the whole scanned  $2\theta$  range. Intensities used in Eq. (1) are corrected for Lorentz-polarization factor, and x-ray absorption is neglected.

<sup>a)</sup>E-mail: komogor@iph.krasn.ru

Magnetic measurements were made by SQUID MPMS (Magnetic Property Measurement System) and VSM PPMS (Physical Property Measurement System) - Quantum Design magnetometers in the fields up to 90 kOe at 5 K and 300 K. The powder sample was fixed in wax matrix to avoid particle displacement in VSM cell. In order to eliminate the effects of thermal fluctuations on the measured value of MAE,<sup>12</sup> we analyze the data measured at 5 K only.

Magnetocrystalline anisotropy in polycrystalline and nanoparticle systems with randomly oriented easy magnetization axes could be investigated via study of approach magnetization to saturation curves. According to Refs. 18–20, the high- and low-field regime for the approach magnetization to saturation law should be distinguished. Magnetization curve in  $H > H_R = 2A/M_s \cdot R_c^2$  range is determined solely by competition between the energy of the external magnetic field and the magnetic anisotropy energy and thus allows to determine the latter from the experimental  $M(H)$  curve by fitting it with Eq. (2) given below.<sup>18–22</sup> Here  $A$  is the exchange constant,  $R_c$  is “structural correlation length” or the average crystallite size  $D = 2R_c$ , and  $M_s$  is saturation magnetization.<sup>20</sup> Using  $A = 1 \times 10^{-6}$  erg/cm,  $M_s = 800$  Gs<sup>1</sup> and the crystallite size from XRD for CoPt particles, we obtain for the samples  $H_R < 6$  kOe ( $D > 10$  nm). Thus, performing measurements in the fields close to 50 kOe (by MPMS) and close to 90 kOe (by PPMS), we are working in the high-field regime. According to the approach to saturation law in the high-field regime  $M(H)$  curve behaves as<sup>18–20</sup>

$$M(H) = M_s [1 - (C/H)^2], \quad (2)$$

where  $C = aH_a$  is the product of magnetic anisotropy field of crystallite or nanoparticle  $H_a$  and coefficient  $a$  which depends on whether nanoparticle has uniaxial or cubic anisotropy.<sup>18</sup>

We have to discuss whether the applied field (up to 90 kOe) is enough for using Eq. (2) which is obtained in the limit of  $H \gg H_a$ , taking into account that for CoPt  $L1_0$  fully ordered phase  $H_a(L1_0) \approx 120$  kOe. Figure 1 shows that reversible part of well-known Stoner-Wohlfarth magnetization

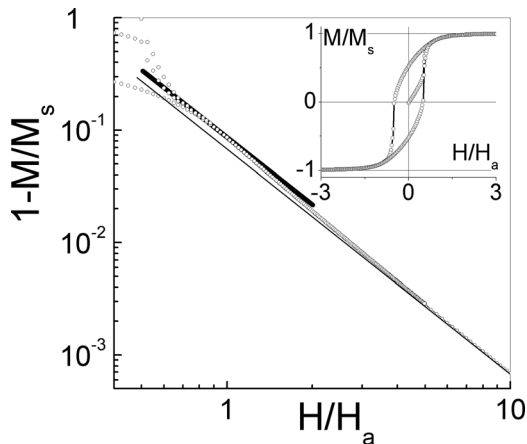


FIG. 1. Approach magnetization to saturation curve for Stoner-Wohlfarth particles with randomly oriented easy axis. Inset shows hysteresis loop for Stoner-Wohlfarth particles. Thin solid line represents Eq. (2) with  $C = (1/15)^{1/2} H_a$ . Bold black line represents Eq. (2) with corrected  $C$  coefficient.

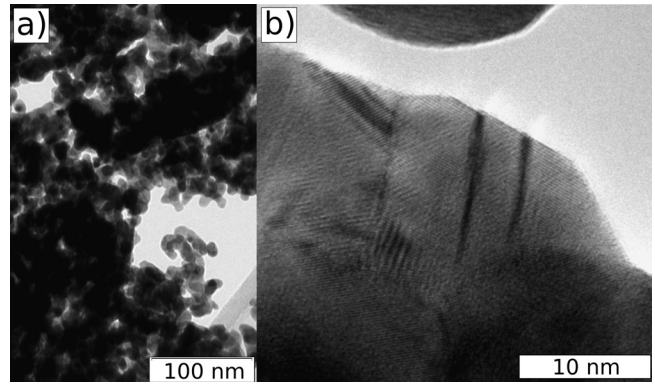


FIG. 2. TEM images for (a) as-decomposed and (b) annealed at 400°C for 2 h CoPt nanostructured particles.

curve for particles with random orientations of easy magnetization axes<sup>29</sup> is described by Eq. (2) for the fields  $H > 3 H_a$ . In the case when applied fields are in the range  $(0.7-1) H_a$  (that approximately corresponds to our case) magnetization curve could be fitted by  $M \sim H^{-2}$  too (bold line in Fig. 1). Thus we correct  $C$  obtained from fitting  $M(H)$  in the fields between  $0.7 S \cdot H_a(L1_0)$  and  $S \cdot H_a(L1_0)$  by the factor of 1.12 to offset the shift of the bold line in Fig. 1.

Individual particle of the as-decomposed CoPt powder is sponge-like agglomerate of crystallites with size about 10 nm (Fig. 2(a)). The annealing of CoPt powder results in growth of crystallites and formation of several distinguished nucleation sites inside single crystallite (Fig. 2(b)). According to XRD patterns (Fig. 3) as-prepared CoPt nanoparticles are characterized by disordered fcc structure. Superlattice reflections appear and grow on XRD patterns during annealing (Fig. 3).

The hysteresis loop is significantly transformed by the annealing (Fig. 4). The increase in value of the coercive

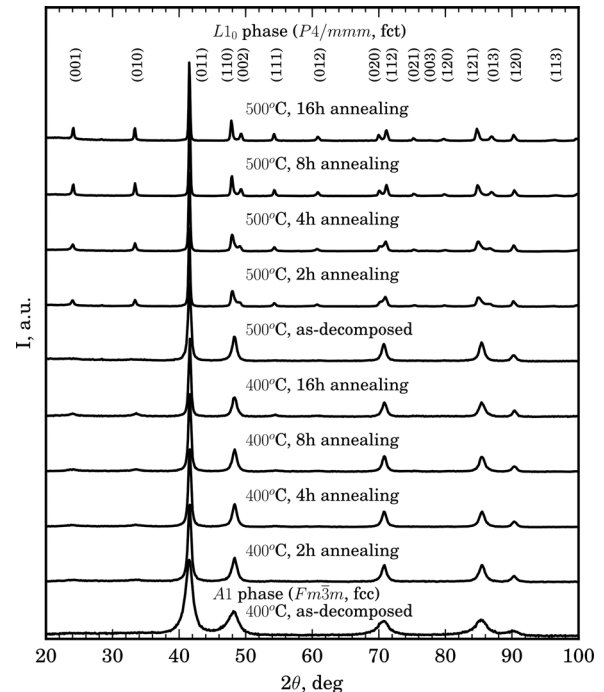


FIG. 3. X-ray powder diffraction patterns for as-decomposed and annealed CoPt nanostructured particles.

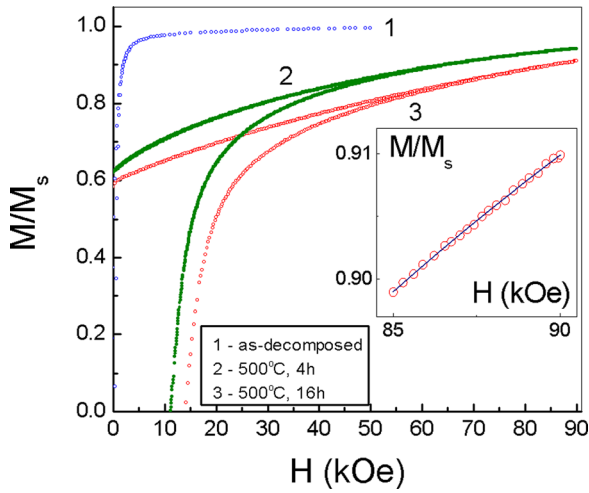


FIG. 4. Hysteresis loops for as-decomposed and annealed CoPt nanostructured particles at 5 K. Inset: the magnetization curve fitting by Eq. (2) for the CoPt particles annealed at 500 °C for 16 h.

force during annealing (from 0.4 kOe in as-decomposed sample up to 14.5 kOe after annealing at 500 °C for 16 h) for the investigated CoPt samples is caused by formation of the  $L1_0$  regions.

Parameter  $C$  obtained from fitting  $M(H)$  by Eq. (2) is  $C = (1/15)^{1/2}H_a$  for uniaxial and  $(2/105)^{1/2}H_a$  for cubic anisotropy.<sup>18,20</sup> In the case of the investigated particles there are both uniaxial and cubic contributions in MAE for  $L1_0$  and A1 regions, respectively. The expression for the combined magnetic anisotropy case  $C = [1/15 \cdot (f \cdot H_a(L1_0))^2 + 2/105((1-f) \cdot H_a(A1))^2]^{1/2}$  should be used where  $f$  is the fraction of the ordered phase.<sup>30–33</sup> Given that  $H_a(L1_0) \gg H_a(A1)$  we obtain  $C \approx (1/15)^{1/2}H_a = (1/15)^{1/2}H_a(L1_0)f$ . The effective magnetic anisotropy constant is calculated as  $K = H_a \cdot M_s / 2 = C \cdot M_s \cdot 15^{1/2} / 2 \cdot 24$ , where  $M_s$  is assumed to be 800 G as in the bulk crystal.<sup>1</sup> We have determined the MAE by the fitting  $M(H)$  curve with the approach magnetization to saturation law in the field range 85–90 kOe (see inset in Fig. 4), i.e., in the high-field regime Eq. (2) that corresponds to the averaging of MAE inside regions with the size below 10 nm,<sup>20</sup> being close to the size of crystallite. Thus the estimated MAE corresponds to the single crystallite.

Assuming homogeneous partially ordered  $L1_0$  phase spreading over the whole crystallite the experimental points in Fig. 5 should be consistent with the curve  $K = K(L1_0) \cdot S^2$  ( $K(L1_0) = 4.7 \times 10^7$  erg/cm<sup>3</sup>), but that is not the case. We then examine more realistic model of the CoPt powder containing both ordered  $L1_0$  and disordered A1 regions. There are several distinguished nucleation sites in one crystallite (Fig. 2(b)). It has been experimentally shown that even 2–10 nm sized CoPt nanocrystal can contain several  $L1_0$  regions.<sup>34–36</sup> Taking into account the size of our crystallites about 10 nm, we consider the existence of several c-domains with different c-axis directions inside single crystallite to be a plausible assumption. In this case experimentally determined order parameter  $S$  depends both on the fraction of the ordered phase ( $f$ ), and the degree of the solid solution ordering in the tetragonal  $L1_0$  domains ( $S_{order}$ ):  $S = f \cdot S_{order}$ .<sup>17</sup> It is established for FePt particles that the magnitude and major changes in the average order

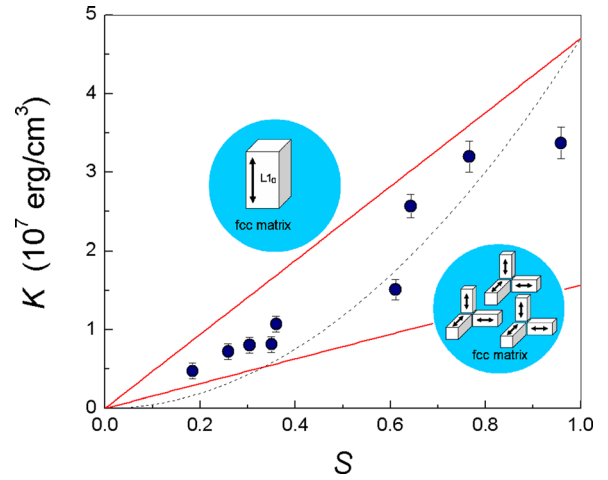


FIG. 5. Magnetic anisotropy energy at 5 K in a crystallite of nanostructured CoPt particles with different degree of ordering.

parameter  $S$  during annealing are associated mostly with the changes of the fraction of the ordered phase ( $f$ ) while  $S_{order} \approx 1$  and remains almost constant during structural transformations.<sup>17</sup> Therefore, we assume  $S = f$ . We then consider two extreme cases: one or many completely ordered  $L1_0$  domains inside disordered fcc matrix.

In the first case  $K = K(L1_0) \cdot S$  (Fig. 5 top straight line).<sup>12</sup> Points lying below line  $K = K(L1_0) \cdot S$  are assumed to correspond to the presence of several c-domains of  $L1_0$  phase in CoPt particles. It was shown that if there are multiple  $L1_0$  domains oriented along one of the three orthogonal axes of the initial fcc structure, with the full conversion from A1 to  $L1_0$ , one should expect the magnetic anisotropy to be  $K(L1_0)/3$ .<sup>12</sup> In the second case  $K = K(L1_0) \cdot S/3$  (Fig. 5 bottom straight line). This result is obtained under the assumption that the volume fraction of  $L1_0$  domains occupying each of the 3 possible orientations is the uniformly distributed random number. This assumption is plausible if large number of  $L1_0$  domains is located inside nanoparticle. Intermediate case, when the particle has few  $L1_0$  domains imply dependence  $K = K(L1_0) \cdot S \cdot \varphi$ , where  $\varphi$  is ranging from 1 to 1/3. This clarifies the distribution of data points in Figure 5 between the top and bottom lines and means that the crystallites of the studied CoPt particles contain few  $L1_0$  domains.

To sum up, we have experimentally shown that the effective MAE value of a crystallite in CoPt partially ordered nanostructured particles could be represented as an intermediate case between two extremes, corresponding to the existence of either single or several c-domains of  $L1_0$  phase in crystallite.

The authors are grateful to Dr. A. V. Zadesenets for synthesis of CoPt complex precursor and Dr. A. S. Bogomyakov for assistance in magnetic measurements. The work was supported by RFBR (Grant Nos. 11-03-00168-a and 12-02-00943-a), Interdisciplinary integration of fundamental research of SB RAS (2012–2014) project No. 64, and grant of the President of the Russian Federation (No. MK-1934.2013.3).

<sup>1</sup>J. M. D. Coey, *Magnetism and Magnetic Materials* (Cambridge University Press, New York, 2010).



- <sup>2</sup>R. C. O'Handley, *Modern Magnetic Materials: Principles and Applications* (Wiley-Interscience, New York, 1999).
- <sup>3</sup>I. Kaitsu, H. Sato, and I. Okamoto, U.S. patent 6,562,481 (2003).
- <sup>4</sup>O. Hellwig, J. S. Lille, A. T. McCallum, O. Mosendz, and D. K. Weller, U.S. patent 8,399,051 (2013).
- <sup>5</sup>M. L. Plumer, J. Van Ek, and D. Weller, *The Physics of Ultra-High-Density Magnetic Recording* (Springer-Verlag, Berlin/Heidelberg, 2001), Vol. 41.
- <sup>6</sup>F. Tournus, A. Tamion, N. Blanc, A. Hannour, L. Bardotti, B. Prével, P. Ohresser, E. Bonet, T. Epicier, and V. Dupuis, *Phys. Rev. B* **77**, 144411 (2008).
- <sup>7</sup>F. Tournus, N. Blanc, A. Tamion, M. Hillenkamp, and V. Dupuis, *J. Magn. Magn. Mater.* **323**, 1868 (2011).
- <sup>8</sup>C. Petit, S. Rusponi, and H. Brune, *J. Appl. Phys.* **95**, 4251 (2004).
- <sup>9</sup>A. Demortière and C. Petit, *J. Appl. Phys.* **109**, 084344 (2011).
- <sup>10</sup>R. K. Rakshit and R. C. Budhani, *J. Phys. D: Appl. Phys.* **39**, 1743 (2006).
- <sup>11</sup>X. Sun, Z. Y. Jia, Y. H. Huang, J. W. Harrell, D. E. Nikles, K. Sun, and L. M. Wang, *J. Appl. Phys.* **95**, 6747 (2004).
- <sup>12</sup>N. A. Usov and J. M. Barandiaran, *Appl. Phys. Lett.* **101**, 172402 (2012).
- <sup>13</sup>V. V. Maykov, A. Y. Yermakov, G. V. Ivanova, V. I. Khrabrov, and L. M. Magat, *Phys. Met. Metallogr.* **67**, 76 (1989).
- <sup>14</sup>J. M. MacLaren, R. R. Duplessis, R. A. Stern, and S. Willoughby, *IEEE Trans. Magn.* **41**, 4374 (2005).
- <sup>15</sup>A. Alam, B. Kraczek, and D. D. Johnson, *Phys. Rev. B* **82**, 24435 (2010).
- <sup>16</sup>R. A. Ristau, K. Barmak, L. H. Lewis, K. R. Coffey, and J. K. Howard, *J. Appl. Phys.* **86**, 4527 (1999).
- <sup>17</sup>M. F. Toney, W. Y. Lee, J. A. Hedstrom, and A. Kellock, *J. Appl. Phys.* **93**, 9902 (2003).
- <sup>18</sup>V. A. Ignatchenko, R. S. Iskhakov, and G. V. Popov, *Sov. Phys. JETP* **55**, 878 (1982).
- <sup>19</sup>E. M. Chudnovsky, W. M. Saslow, and R. A. Serota, *Phys. Rev. B* **33**, 251 (1986).
- <sup>20</sup>R. S. Iskhakov and S. V. Komogortsev, *Phys. Met. Metallogr.* **112**, 666 (2011).
- <sup>21</sup>Y. Melikhov, J. E. Snyder, D. C. Jiles, A. P. Ring, and J. A. Paulsen, *J. Appl. Phys.* **99**, 08R102 (2006).
- <sup>22</sup>A. Franco, F. L. A. Machado, and V. S. Zapf, *J. Appl. Phys.* **110**, 053913 (2011).
- <sup>23</sup>A. Zadesenets, E. Filatov, P. Plyusnin, I. Baidina, V. Dalezky, Yu. Shubin, S. Korenev, and A. Bogomyakov, *Polyhedron* **30**, 1305 (2011).
- <sup>24</sup>G. Caglioti, A. T. Paoletti, and F. P. Ricci, *Nucl. Instrum.* **3**, 223 (1958).
- <sup>25</sup>M. Wojdyr, *J. Appl. Cryst.* **43**, 1126 (2010).
- <sup>26</sup>P. Scardi and M. Leoni, *Acta Crystallogr. A* **58**, 190 (2002).
- <sup>27</sup>M. Leoni, T. Confente, and P. Scardi, *Z. Kristallogr. Suppl.* **23**, 249 (2006).
- <sup>28</sup>S. V. Komogortsev, N. A. Chizhik, E. Yu. Filatov, S. V. Korenev, Yu. V. Shubin, D. A. Velikanov, R. S. Iskhakov, and G. Yu. Yurkin, *Solid State Phenom.* **190**, 159 (2012).
- <sup>29</sup>E. C. Stoner and E. P. Wohlfarth, *Philos. Trans. R. Soc. London, Ser. A* **240**, 559 (1948).
- <sup>30</sup>J. Geshev, M. Mikhov, and J. E. Schmidt, *J. Appl. Phys.* **85**, 7321 (1999).
- <sup>31</sup>J. Geshev, A. D. C. Viegas, and J. E. Schmidt, *J. Appl. Phys.* **84**, 1488 (1998).
- <sup>32</sup>S. I. Smirnov and S. V. Komogortsev, *J. Magn. Magn. Mater.* **320**, 1123 (2008).
- <sup>33</sup>N. A. Usov and J. M. Barandiaran, *J. Appl. Phys.* **112**, 053915 (2012).
- <sup>34</sup>C. Frommen and H. Rösner, *Mater. Lett.* **58**, 123 (2004).
- <sup>35</sup>F. Tournus, K. Sato, T. Epicier, T. J. Konno, and V. Dupuis, *Phys. Rev. Lett.* **110**, 055501 (2013).
- <sup>36</sup>K. Sato, K. Yanajima, and T. J. Konno, *Thin Solid Films* **520**, 3544 (2012).